PHYSICAL REVIEW B **87**, 161115(R) (2013)

Anomalous electron trajectory in topological insulators

Li-kun Shi,[1] Shou-cheng Zhang,[2] and Kai Chang[1,*]
[1]*SKLSM, Institute of Semiconductors, Chinese Academy of Sciences, P.O. Box 912, Beijing 100083, China*
[2]*Department of Physics, Stanford University, Stanford, California 94305, USA*
(Received 23 October 2012; published 22 April 2013)

We present a general theory about electron orbital motions in topological insulators. An in-plane electric field drives spin-up and spin-down electrons bending to opposite directions, and skipping orbital motions, a counterpart of the integer quantum Hall effect, are formed near the boundary of the sample. The accompanying Zitterbewegung can be found and controlled by tuning external electric fields. Ultrafast flipping electron spin leads to a quantum side jump in the topological insulator, and a snake-orbit motion in two-dimensional electron gas with spin-orbit interactions. This feature provides a way to control electron orbital motion by manipulating electron spin.

DOI: 10.1103/PhysRevB.87.161115 PACS number(s): 71.70.Ej, 72.25.Mk, 75.76.+j

The time-reversal invariant topological insulator (TI) is a new state of quantum matter possessing insulating bulk and metallic edge or surface states, which show a linear massless Dirac dispersion.[1,2] TIs are distinguished from a normal band insulator by a nontrivial topological invariant Z_2 characterizing its band structure. The quantum spin Hall effect was proposed in graphene[3] and HgTe quantum wells.[4] The existence of edge and surface states was confirmed by a recent experiment in HgTe quantum wells[5] and angle-resolved photoemission spectroscopy experiments.[6,7] Due to its unique band structure, TI is a good testbed for observing relativistic effects, predicted by the Dirac equation, as, for instance, the Klein's paradox and Zitterbewegung (ZB).

So far, most previous works in the rapidly growing field of TIs focused on exploring new TIs and their transport and magnetic properties. Relatively, electron dynamics in TIs is unexplored. In this Rapid Communication we show that the quantum spin Hall effect and quantum anomalous Hall effect[8] can be understood from anomalous electron orbital motions in TIs. These anomalous electron orbital motions in topological insulators naturally give a clear picture about the origin of the edge states, a counterpart of the skipping orbital motion in the integer quantum Hall effect. By applying a series of magnetic field pulses to flip electron spin quickly, a quantum side-jump behavior and a snake-orbit motion can be found for electrons in TIs and normal 2DEG with spin-orbit interactions (SOIs), respectively. The trembling motion, i.e., the ZB, can be controlled by changing an in-plane electric field and the initial momentum of the electron wave packet.

We consider the single-particle Hamiltonian of the electron at a low-energy regime in the presence of a uniform electric field $\boldsymbol{E}$,

$$\begin{aligned} H &= H_0(k) + V(\boldsymbol{r}) \\ &= \epsilon(k)I + \sum_{i=1}^{3} d_i^0(k)\sigma_i - e\boldsymbol{E}\cdot\boldsymbol{r}, \end{aligned} \tag{1}$$

where σ_i ($i = 1,2,3$) is the Pauli matrix and $\epsilon(k)$ is the kinetic energy. The different forms of d_i can be used to describe the various important systems: (1) two-dimensional electron gas with Rashba and Dresselhaus SOIs with $d_1^0 = -\alpha k_y - \beta k_x$, $d_2^0 = \alpha k_x + \beta k_y$, $d_3^0 = 0$, where α and β describe the strengths of Rashba and Dresselhaus SOIs, respectively;[9] (2) single layer graphene with $d_1^0 = v_F\hbar k_x$, $d_2^0 = v_F\hbar k_y$, $d_3^0 = 0$;[10] (3) bilayer graphene with $d_1^0 = -\hbar^2(k_x^2 - k_y^2)/2m$, $d_2^0 = -\hbar^2 k_x k_y/m$, $d_3^0 = 0$;[10] (4) two-dimensional TI HgTe quantum wells with an inverted band structure with $d_1^0 = Ak_x$, $d_2^0 = Ak_y$, $d_3^0 = M - Bk^2$;[4] and (5) three-dimensional TIs, e.g., Bi_2Se_3 and Bi_2Te_3, whose Hamiltonian would be extended to $H = \sum_{\mu,\nu=0}^{3} d_{\mu\nu}^0(k)\sigma_\mu \otimes \sigma_\nu - e\boldsymbol{E}\cdot\boldsymbol{r}$, in which $\sigma_0 = I_{2\times 2}$, and $d_{00}^0 = \epsilon(k)$, $d_{03}^0 = M(k)$, $d_{31}^0 = A_1 k_z$, $d_{11}^0 = A_2 k_x$, $d_{12}^0 = A_2 k_y$ while other $d_{\mu\nu}^0$'s are zero.[11,12]

In the absence of a uniform electric field, the electron position operator $y_H(t)$ evolving with the time t can be obtained as

$$\begin{aligned} y_H(t) &= e^{iHt/\hbar} y e^{-iHt/\hbar} \\ &= y(0) + (it/\hbar)[H,y] + \frac{(it/\hbar)^2}{2!}[H,[H,y]] + \cdots \\ &= y(0) + (it/\hbar)\epsilon^y + \sum_{n=1}\frac{(it/\hbar)^n}{n!}T_n, \end{aligned} \tag{2}$$

where $\epsilon^y = [\epsilon,y] = -i\,\partial_{k_y}\epsilon$, $D^0 = \sum_j d_j^0\sigma_j$, $T_1 = [D^0,y] = \sum_j d_j^y\sigma_j = D^y$, $T_2 = [D^0,D^y] = \sum_{i,j} d_i^0 d_j^y[\sigma_i,\sigma_j]$, ..., the nth commutator $T_n = [D^0,T_{n-1}]$. Generally, the analytical expression of the above summation is very difficult to obtain because the number of commutators increases hierarchically with increasing the order n.

Interestingly, the equivalence between the commutation relationship $[\sigma_i,\sigma_j] = 2i\varepsilon_{ijk}\sigma_k$ and the vector cross production $(\boldsymbol{A}\times\boldsymbol{B})_k = \varepsilon_{ijk}A_iB_j\mathbf{e}_k$ (Ref. 13) offers us a way to solve this problem. In the absence of an external electric field, the commutation between the spin operators is converted into the vector product between them. We can transfer the algebra summation in Eq. (2) into the summations of the vector series $T_{2n+1}(T_{2n})$ ($n = 1,2,\ldots$) by utilizing the equivalence between the commutator $[D^0,T_n]$ and the vector product $D^0 \times T_n$, $T_n = [D_0,T_{n-1}] \sim 2i(D^0 \times T_{n-1})$.[13] One can see that the vectors T_{2n} and T_{2n+1} ($n = 0,1,2,\ldots$) point along the orthogonal directions while the lengths of the vectors T_n vary with an increase of the order n as $T_{2n+1} = -|2D^0|^2 T_{2n-1}$, where $|D_0| = [\sum_{i=1}^{3}(d_i^0)^2]^{1/2}$. This character allows us to get

the analytical expression for the electron position operator,

$$y_H(t) = y(0) + \frac{it}{\hbar}\left(\epsilon^y + T_1 - \frac{T_3}{|D^0|^2}\right) + \frac{T_2}{2|D^0|^2}[\cos(2|D^0|t/\hbar) - 1] + \frac{iT_3}{2|D^0|^3}[\sin(2|D^0|t/\hbar)]. \quad (3)$$

This analytical expression consists of the initial position (the first term), the propagating term (the second term), and the *Zitterbewegung* term (the last two terms). This ZB term describes the rapid trembling motion which has no the classical correspondences. ZB, a novel relativistic quantum orbital motion, is an inherent hallmark of the Dirac equation, first predicted by Schrödinger in 1930.[14] This rapid quivering motion of the electron arises from the superposition between the positive- and negative-energy part of the spinor states and could be a possible origin of the electron spin.[15] Although there are many proposals about the observation of the ZB in a two-dimensional electron gas (2DEG) with SOIs,[9,16] graphene,[10] a Cooper pair in superconductors,[17,18] and general theoretical analysis,[19] this phenomenon has only been observed experimentally in the trapped ion[20–22] and cold atom[23] systems. However, this prediction still needs to be observed for electrons in free space; this is because the ZB displays an extremely high frequency, $\omega_Z = 2m_0c^2/\hbar \approx 1.5 \times 10^{21}$ Hz, and a tiny amplitude, $\lambda_Z = \hbar/m_0c \approx 3.9 \times 10^{-4}$ nm (m_0 is the electron mass). The detection of the oscillation with such a high frequency and negligibly small amplitude is beyond the reach of the present-day experimental technique.

It is natural to imagine that the frequency of the ZB should be decreased when the energy gap decreases. TI could be a good testbed to observe the ZB due to its narrow bulk gap, which ranges from 10 meV to 0.3 eV. The expression of ZB [see Eq. (3)] agrees exactly with previous theoretical works for various systems. For a 2DEG with Rashba and Dresselhaus SOIs,[9] $\epsilon^y + T_1 = -i\hbar^2 k_x/m - i(\alpha\sigma_y - \beta\sigma_x)$, $T_2 = (\alpha^2 - \beta^2)k_y\sigma_z$, $T_3 = (\alpha^2 - \beta^2)(k_x\sigma_y - k_y\sigma_x)\Sigma$, where $\Sigma = \alpha(k_x\sigma_x + k_y\sigma_y) + \beta(k_x\sigma_y + k_y\sigma_x)$, $|D^0| = (\alpha^2 + \beta^2)k^2 + 4\alpha\beta k_x k_y$. For a single layer graphene,[10] $\epsilon^y + T_1 = -i\hbar v_F\sigma_x$, $T_2 = \hbar^2 v_F{}^2 k_y\sigma_z$, $T_3 = \hbar^3 v_F{}^3 k_y(k_x\sigma_y - k_y\sigma_x)$, $|D^0| = v_F\hbar k$. The two-dimensional TI HgTe quantum wells with an inverted band structure,[4] $\epsilon^y + T_1 = -i(2Dk_y + A\sigma_y)$, $T_2 = -2A(M - Bk^2)\sigma_x + 2A^2 k_x\sigma_z$, $T_3 = 4i\{A^3 k_x k_y\sigma_x - [A(M - Bk^2)^2 + A^3 k_x^2]\sigma_y + A^2(M - Bk^2)k_y\sigma_z\}$ [see Fig. 1(a)]. The second term, $\epsilon^y + T_1 - T_3/|D^0|^2$, represents the classical uniform rectilinear motion, and the third and the fourth terms T_2 and T_3 describe the ZB with an oscillating frequency $2|D^0|/\hbar$. The trembling frequency is determined by the strength of the spin-orbit interaction of the interband coupling d_i^0. For all of the above examples, these agreements demonstrate the validity of the diagram technique developed by us.

In two-terminal transport experiments, an external voltage is applied between the source and drain, generating an in-plane electric field. In the presence of a uniform in-plane electric field, it is difficult to get the analytical expression of the electron position operator as discussed above. Instead, we can

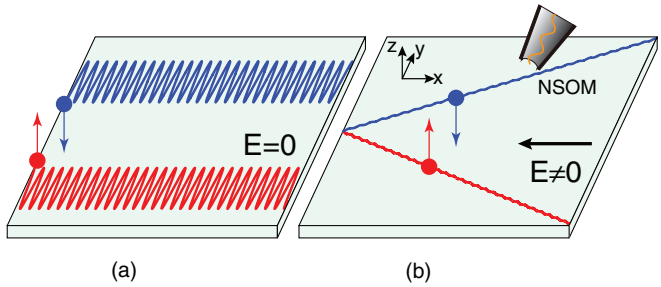

FIG. 1. (Color online) Schematic of electron orbital motion in a HgTe quantum well with an inverted band without and with an in-plane driving electric field [(a) and (b)]. The orbital motion can be detected by the optical technique, e.g., the NSOM at the microwave frequency regime.

calculate the electron position $\mathbf{r}(t)$ based on the equation of motion $i\hbar\dot{\mathbf{r}} = [\mathbf{r}, H]$. We consider a two-dimensional topological insulator, a HgTe quantum well with an inverted band structure described by the Bernevig-Hughes-Zhang (BHZ) model.[4] The single-particle effective Hamiltonian for the electron is

$$H(k)_{\uparrow\downarrow} = H_0(k)_{\uparrow\downarrow} + V(x_i), \quad (4)$$

where $H_0(k)_{\uparrow\downarrow} = C - Dk^2 \pm Ak_x\sigma^x + Ak_y\sigma^y + (M - Bk^2)\sigma^z$, $V(\mathbf{x}) = -e\mathbf{E}\cdot\mathbf{r}\sigma^z$. A, B, C, D, and M are the parameters determined by the thickness of the quantum well.[24] Consider an electron injected in the Gaussian wave packet $\varphi(r) = \frac{1}{2\pi}\frac{d}{\sqrt{\pi}}\int d^2k e^{-d^2(\vec{k}-\vec{k}_0)^2/2} e^{i\vec{k}\cdot\vec{r}}\,|\uparrow\rangle$ with the spatial width $(\Delta x)^2 = (\Delta y)^2 = d^2/2$ and spin pointing along the z axis, perpendicular to the quantum well plane. The guiding center of the wave packet $\langle y_H(t)\rangle$ can be calculated numerically by the Heisenberg equation of motion $d\langle y_H(t)\rangle/dt = (ih)^{-1}\langle[y_H(t), H]\rangle$. From the numerical results (the red and blue curves in Fig. 2), the spin-up and spin-down electrons driven by an in-plane electric field E_x bend to the opposite direction along the y axis, accompanied

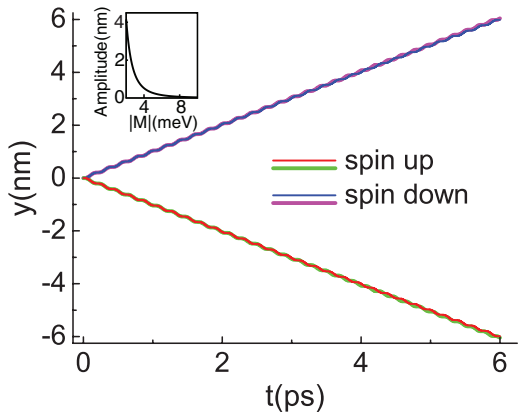

FIG. 2. (Color online) The trajectories of spin-up (the red and green curves) and spin-down (the blue and purple curves) electrons incident with an initial momenta $k_{x0} = 0.001$ nm^{-1}, and the electric field $E_x = 10$ V/cm. The red and blue (green and purple) curves denote the numerical (analytical) results. The parameters used in the calculation are adopted from Ref. 24. The inset shows the amplitude of the transverse ZB, y^{ZB}, as a function of the bulk gap of the HgTe quantum well (QW), $|M|$.

by a trembling behavior, i.e., the ZB. Notice that the electron energy $\langle E\rangle = C + M - (B+D)/d^2 - (B+D)k_0^2$ locates in the bulk gap, which is the important difference from the spin Hall effect in a conventional 2DEG and/or metal with SOIs.

In order to understand this surprising feature, we analyze the equation of motion utilizing the adiabatic approximation, i.e., separating the fast trembling motion and slow orbital motion $y_{\uparrow\downarrow} = y^{\rm orb}_{\uparrow\downarrow} + y^{\rm ZB}_{\uparrow\downarrow}$.[25,26] First we perform a unitary transformation $U(k)$ to diagonalize the Hamiltonian $H_0(k)$, i.e., $\tilde{H}_0 = U(k)_{\uparrow\downarrow} H_0(k)_{\uparrow\downarrow} U^\dagger(k)_{\uparrow\downarrow}$. The potential term becomes $V(\tilde{D}_i)$, where the covariant derivative $\tilde{D}_i = i\partial_{k_i} - \tilde{A}_i$, and $\tilde{A}_i(k)_{\uparrow\downarrow} = -i\cdot U(k)_{\uparrow\downarrow}\partial_{k_i} U^\dagger(k)_{\uparrow\downarrow} \cdot U(k)_{\uparrow\downarrow}\sigma^z U^\dagger(k)_{\uparrow\downarrow}$ behaves as a gauge field. Adopting the adiabatic approximation, i.e., neglecting the off-diagonal matrix elements of $\tilde{A}_i$, the resulting gauge field A_i only contains a diagonal matrix which gives a nonzero associated field strength $F_{ij} = i[D_i, D_j]$, where $x_i \to D_i = i\partial_{k_i} - A_i$, and then the effective Hamiltonian becomes

$$H^{\rm eff}_{\uparrow\downarrow} = \tilde{H}_0(k) - e\sum_{i=x,y} E_i D_{i,\uparrow\downarrow}, \tag{5}$$

where $\tilde{H}_0(k) = C - Dk^2 - \sqrt{A^2k^2 + (M - Bk^2)^2}\sigma^z$ for both spin-up (down) states. The nontrivial property of the Hamiltonian is revealed through the nontrivial commutation relations $[k_i, k_j] = 0$, $[D_i, k_j] = i\delta_{ij}$, $[D_i, D_j] = -iF_{ij}$, and the effective "Lorentz forces" in momentum space felt by spin-up or spin-down electrons is

$$F_{xy}(k)_{\uparrow\downarrow} = \pm\frac{A^2(M^2 - B^2k^4)}{2[A^2k^2 + (M - Bk^2)^2]^2}.$$

The equation of motion for the spin-up and spin-down electrons can be written as

$$\begin{aligned} \dot{x}_{\uparrow\downarrow} &= u_x \pm |F_{xy}|\,\dot{k}_y, \\ \dot{y}_{\uparrow\downarrow} &= u_y \mp |F_{xy}|\,\dot{k}_x, \\ k_i &= k_{i0} + \lambda e E_i t/\hbar, \end{aligned} \tag{6}$$

where u_i represents the usual group velocity $\partial\tilde{H}_0/\partial k_i$, and $\lambda = \pm 1$ stands for the negative (positive) branch of the energy spectrum. When $k_{y0} = 0$, the orbital trajectory of a spin-up or spin-down electron at small k is[13]

$$y^{\rm orb}_{\uparrow\downarrow} = \mp\frac{A^2}{2M^2}k_x + O(k)^3. \tag{7}$$

Clearly, one can see that the spin-up and spin-down electrons feel an opposite force $F_{xy}(k)_{\uparrow\downarrow}$, respectively, which pushes them against the opposite direction. The trajectories are obtained from Eq. (7), which neglects the fast trembling motion by the adiabatic approximation. The analytical expression for the trembling motion, i.e., the ZB, at small k can also be obtained:[13]

$$y^{\rm ZB}_{\uparrow\downarrow} = \pm\frac{A^2}{2M^2}\frac{eE_x}{\Delta\epsilon(t)}\sin\left(\frac{\Delta\epsilon(t)}{\hbar}t\right), \tag{8}$$

where $\Delta\epsilon(t) = 2\sqrt{A^2k^2 + (M - Bk^2)^2} = 2|M| + O(k^2)$. At small in-plane momentum k, the kinetic energy can be neglected, and the frequency of amplitude of the ZB is determined by M, the gap of the HgTe QW which can be tuned by the thickness of the QW. The total electron trajectories

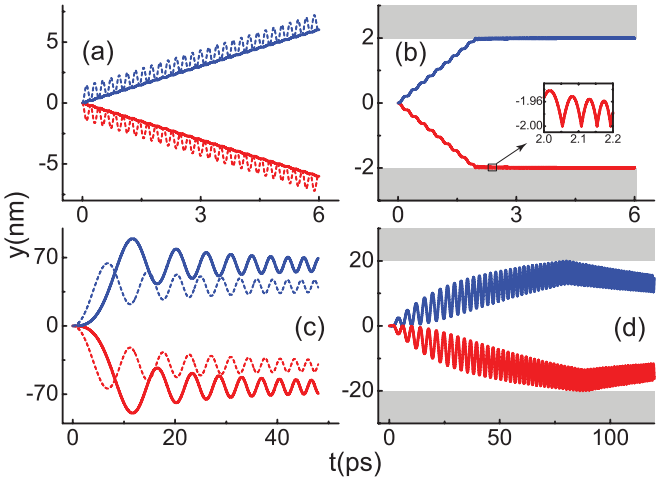

FIG. 3. (Color online) The trajectories of spin-up (red) and spin-down (blue) incident electrons under a uniform electric field. The in-plane electric field $E = 10$ V cm^{-1}. The electron injected into a HgTe quantum well ($M = -10$ meV) (a) has a initial incident momentum $k_{x0} = 0$ for the solid curves and $k_{x0} = 0.001$ nm^{-1} for the dashed curves. (b) The same as (a), but with a hard-wall boundary (the shaded regions). The inset amplifies the trajectory near the boundary, showing the skipping orbital motion. (c), (d) The same as (a) and (b), but in a conventional GaAs 2DEG with a Rashba spin-orbit interaction ($\alpha = 10$ meV nm taken from Ref. 4). The solid and dashed curves correspond to $k_{x0} = 0$ and $k_{x0} = 0.01$ nm^{-1}, respectively.

$y_{\uparrow\downarrow} = y^{\rm orb}_{\uparrow\downarrow} + y^{\rm ZB}_{\uparrow\downarrow}$ obtained from Eqs. (7) and (8) agree well with the numerical results for spin-up and spin-down electron incident cases (see Fig. 2). The inset in Fig. 2 shows that the amplitude of the ZB increases rapidly with decreasing the gap $|M|$ of the HgTe QW with an inverted band, and a linear dependence on the strength of the in-plane electric field E_x. For example, the amplitude of the ZB is about 21.2 Å when $M = 2.5$ meV and $E_x = 10$ V cm^{-1}, which are within the reach of the state-of-art experimental techniques. By adjusting the electric fields E_x and the bulk gap of HgTe QWs, one can tune the amplitude of the ZB significantly [see Fig. 3(a) and make it possible to observe it in TIs.

For the realistic experimental sample, we need to consider the boundary effect, for instance, a spin Hall bar with a finite width. The spin-up and spin-down electrons will bend to the opposite edges. Figure 3(b) shows clearly that spin-up and spin-down edge states appear near the opposite boundaries of the sample (the shaded regions). From the inset, one can see the skipping orbital motion of electrons in the edge states, since electrons bending to the edges will be bounced back when they hit the hard-wall boundary,[27] and pushed to the boundary again by the driving force (or the effective "Lorentz" force) $F_{xy}(k)_{\uparrow\downarrow}$. This is a counterpart of the skipping orbital motion in the integer quantum Hall effect, but spin-up and spin-down electrons feel the opposite effective "Lorentz" forces, while in a normal 2DEG with SOIs, spin-up and spin-down electrons show a ballistic side jump in opposite directions, which was already found before,[16] but no edge states can be found near the sample boundary. Instead, electrons will oscillate between the opposite boundaries [see Figs. 3(c) and 3(d)].

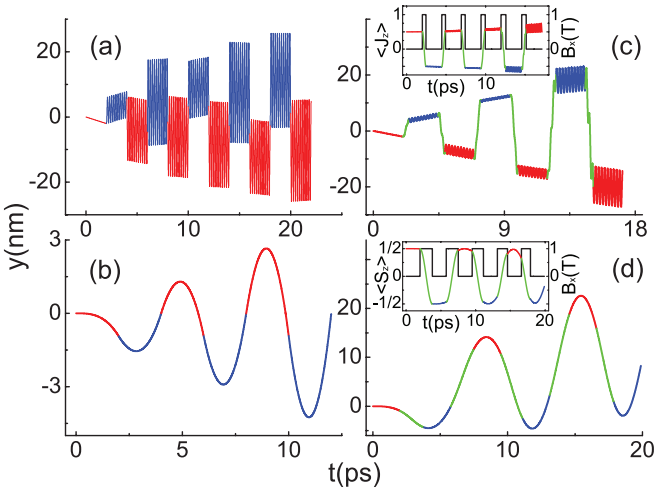

FIG. 4. (Color online) The trajectories of a initial spin-up electron driven by a uniform electric field in HgTe QW (a) and a GaAs 2DEG with SOIs (b). The red and blue curves denote the spin-up and spin-down electrons, respectively. The electron spin is flipped periodically at a time interval $t = 2$ ps. (c), (d) The same as (a) and (b), but for a realistic case: a series of square-shaped magnetic field pulses with the magnitude $B_0 = 1$ T. The parameters are the same as those in Fig. 3, $k_0 = 0$.

Similarly, the quantum anomalous spin Hall effect might be also understood from the electron dynamics in TIs. Considering a ferromagnetic TI, a giant Zeeman splitting results in a spin-up inverted and a spin-down normal band structure; we assume these magnetic ions are polarized along the z axis. This situation corresponds to the BHZ Hamiltonian with positive and negative M for spin-up and spin-down electrons, respectively. From the above discussions, the spin-up (down) electrons show a normal oscillating (bending) trajectory (see Fig. 3). Therefore, the edge states only appear for spin-down electrons, i.e., the quantum anomalous spin Hall effect. Similar behavior can also be found in three-dimensional (3D) topological insulators, because the form of the Hamiltonian of 3D TI is almost the same as that of 2D TI. Therefore one can expect that the bending trajectory of electrons in 3D TIs will lead to topological surface states.

In a spin-orbit system, usually electron spin can be manipulated by controlling its orbital motion, such as a spin transistor.[28] And vice versa, it is also possible to control electron orbital motion by manipulating electron spin. In a 2D TI, e.g., a 2DEG in a HgTe QW with an inverted band structure, electron spin flipping leads to an interesting quantum side jump [see Fig. 4(a)], which is the manifestation of the spin-dependent ZB and is caused by the spin-dependent driving force, while in the 2DEG with SOIs, an interesting snake-orbit motion can be found [see Fig. 4(b)]. This ultrafast spin flipping process can be achieved by applying a series of specifically shaped magnetic field pulses [see the insets in Figs. 4(c) and 4(d)], which was used to flip the magnetization of the magnetic random access memory devices.[29] The width of the magnetic field pulses is determined by the magnitudes of the magnetic field pulses B_0, and usually it will take a longer (shorter) time to flip electron spins for a weak (strong) magnetic field B_0.

Finally, we comment on how to detect these interesting orbital motions experimentally. We propose a near-field scanning optical microscope (NSOM) technique in the microwave or THz regime to detect the edge states, ZB, quantum side jump, and snake-orbit motions. The NSOM technique breaks the far field resolution limit by exploiting the properties of evanescent waves. With this technique, the resolution of the image is limited by the size of the detector aperture and not by the wavelength of the illuminating light. A spatial lateral resolution of the NSOM can approach 20 nm.[30] A microwave light beam is applied at a specific spatial position through a NSOM [see Fig. 1(b)], and the absorption of the microwave beam changes when electrons pass below. This experimental technique was used very recently to detect the topological edge states in a HgTe QW.

In summary, we give an intuitive physical picture about the dynamical origin of the edge states in TIs, a skipping orbit motion. By flipping the electron spin quickly, one can efficiently control the electron orbital motion. An interesting quantum side jump and snake-orbital motion can be found in the TIs and 2DEGs with SOIs. This feature provides a way to control electron orbital motion by manipulating the electron spin.

This work was supported by the NSFC Grants No. 10934007 and No. 2011CB922204 from the MOST of China. S.C.Z. is supported by the DARPA Program on Topological Insulators.

*kchang@semi.ac.cn

[1] X. L. Qi and S. C. Zhang, Phys. Today **63**(1), 33 (2010).
[2] M. Z. Hasan and C. L. Kane, Rev. Mod. Phys. **82**, 3045 (2010).
[3] C. L. Kane and E. J. Mele, Phys. Rev. Lett. **95**, 146802 (2005).
[4] B. A. Bernevig, T. L. Hughes, and S. C. Zhang, Science **314**, 1757 (2006).
[5] M. König, S. Wiedmann, C. Brüne, A. Roth, H. Buhmann, L. W. Molenkamp, X. L. Qi, and S. C. Zhang, Science **318**, 766 (2007).
[6] D. Hsieh, D. Qian, L. Wray, Y. Xia, Y. S. Hor, R. J. Cava, and M. Z. Hasan, Nature (London) **452**, 970 (2008).
[7] Y. L. Chen, J. G. Analytis, J. H. Chu, Z. K. Liu, S. K. Mo, X. L. Qi, H. J. Zhang, D. H. Lu, X. Dai, Z. Fang, S. C. Zhang, I. R. Fisher, Z. Hussain, and Z. X. Shen, Science **352**, 178 (2009).
[8] C. X. Liu, X. L. Qi, Xi Dai, Z. Fang, and S. C. Zhang, Phys. Rev. Lett. **101**, 146802 (2008).
[9] J. Schliemann, D. Loss, and R. M. Westervelt, Phys. Rev. Lett. **94**, 206801 (2005).
[10] T. M. Rusin and W. Zawadzki, Phys. Rev. B **76**, 195439 (2007).
[11] Y. Xia, D. Qian, D. Hsieh, L. Wray, A. Pal, H. Lin, A. Bansil, D. Grauer, Y. S. Hor, R. J. Cava, and M. Z. Hasan, Nat. Phys. **5**, 438 (2009).
[12] H. J. Zhang, C. X. Liu, X. L. Qi, X. Dai, Z. Fang, and S. C. Zhang, Nat. Phys. **5**, 438 (2009).
[13] See Supplemental Material at http://link.aps.org/supplemental/10.1103/PhysRevB.87.161115 for detailed formula derivations.

[14]E. Shrödinger, Sitzungsber. Preuss. Akad. Wiss., Phys.-Math. K1. **24**, 418 (1930).
[15]K. Huang, Am. J. Phys. **20**, 479 (1952).
[16]J. Schliemann, Phys. Rev. B. **75**, 045304 (2007).
[17]F. Cannata, L. Ferrari, and G. Russo, Solid State Commun. **74**, 309 (1990); L. Ferrari and G. Russo, Phys. Rev. B **42**, 7454 (1990); F. Cannata and L. Ferrari, *ibid.* **44**, 8599 (1991).
[18]D. Lurié and S. Cremer, Physica (Amsterdam) **50**, 224 (1970).
[19]R. Winkler, U. Zülicke, and J. Bolte, Phys. Rev. B **75**, 205314 (2007); J. Cserti and G. Dávid, *ibid.* **82**, 201405 (2010); W. Zawadzki and T. M. Rusin, J. Phys. Condens. Matter **23**, 143201 (2011).
[20]L. Lamata, J. León, T. Schätz, and E. Solano, Phys. Rev. Lett. **98**, 253005 (2007).
[21]A. Bermudez, M. A. Martin-Delgado, and E. Solano, Phys. Rev. A **76**, 041801(R) (2007).
[22]R. Gerritsma, G. Kirchmair, F. Zähringer, E. Solano, R. Blatt, and C. F. Roos, Nature (London) **463**, 68 (2010).
[23]J. Y. Vaishnav and C. W. Clark, Phys. Rev. Lett. **100**, 153002 (2008).
[24]M. König, H. Buhmann, L. W. Molenkamp, T. Hughes, C. X. Liu, X. L. Qi, and S. C. Zhang, J. Phys. Soc. Jpn. **77**, 031007 (2008).
[25]S. Murakami, N. Nagaosa, and S. C. Zhang, Science **301**, 1348 (2003).
[26]Z. F. Jiang, R. D. Li, S. C. Zhang, and W. M. Liu, Phys. Rev. B **72**, 045201 (2005).
[27]L. Fu and C. L. Kane, Phys. Rev. Lett. **100**, 096407 (2008); B. Zhou, H. Z. Lu, R. L. Chu, S. Q. Shen, and Q. Niu, *ibid.* **101**, 246807 (2008); E. G. Novik, P. Recher, E. M. Hankiewicz, and B. Trauzettel, Phys. Rev. B **81**, 241303 (2010); K. Chang and W. K. Lou, Phys. Rev. Lett. **106**, 206802 (2011).
[28]S. Datta and B. Das, Appl. Phys. Lett. **56**, 665 (1990); H. C. Koo, J. H. Kwon, J. Eom, J. Chang, S. H. Han, and M. Johnson, Science **325**, 1515 (2009).
[29]Th. Gerrits, H. A. M. van den Berg, J. Hohlfeld, L. Bär, and Th. Rasing, Nature (London) **418**, 509 (2002); M. R. Freeman, R. R. Ruf, and R. J. Gambino, IEEE Trans. Magn. **27**, 4840 (1991).
[30]Y. Oshikane T. Kataoka, M. Okuda, S. Hara, H. Inoue, and M. Nakano, Sci. Technol. Adv. Mater. **8**, 181 (2007).